

## Complex surface alloy formed by Li deposition on Cu(001) determined by dynamical low-energy electron diffraction

Seigi Mizuno and Hiroshi Tochiyama\*

*Catalysis Research Center, Hokkaido University, Kita-ku, Sapporo 060, Japan*

Angelo Barbieri and Michel A. Van Hove

*Materials Sciences Division, Lawrence Berkeley Laboratory, University of California, Berkeley, California 94720*

(Received 2 August 1994)

A detailed structure determination of a complex surface alloy formed by alkali-metal deposition on a metal substrate yields a type of alloy consisting of an ordered assembly of substructures. The  $(3 \times 3)$  structure formed on Cu(001) by Li deposition is found to consist of small pyramids of four Cu atoms capped by single Li atoms, the pyramids being joined by pairs of Li atoms.

Recent studies have revealed that substitutional adsorption or surface alloy formation takes place at room temperature on some metal surfaces upon alkali-metal (AM) adsorption, in contrast to overlayer formation. This was observed on Ag(110), where a  $(1 \times 2)$  reconstruction is formed for Li, K, or Cs adsorption at low coverages.<sup>1</sup> It has been established by low-energy electron diffraction (LEED) and ion beam scattering that a missing-row reconstruction is induced by AM deposition on the fcc(110) surfaces of Cu, Ni, Pd, and Ag.<sup>2</sup> With further AM deposition on the missing-row structures at 300 K, rather complex structures have been observed and proposed to be surface alloys: in particular, a  $c(2 \times 2)$  structure for K/Au(110) (Ref. 3) and  $(4 \times 1)$  and  $(5 \times 1)$  structures for Li/Cu(110).<sup>4</sup>

On fcc(111), an unusual structure was found for Na adsorption on Al(111): a  $(\sqrt{3} \times \sqrt{3})R 30^\circ$  structure is formed at 300 K due to substituted Na atoms in the top Al layer, as determined by surface extended x-ray-absorption fine structure (SEXAFS).<sup>5</sup> It was found for the similar K/Al(111) system at 300 K that the  $(\sqrt{3} \times \sqrt{3})R 30^\circ$  structure is due to substituted K atoms, as analyzed by LEED.<sup>6</sup> In addition to substituted structures,  $(2 \times 2)$  and  $(2\sqrt{3} \times 2\sqrt{3})$  structures were observed at higher coverages for Na/Al(111), and these were suggested to be surface alloys of intermixed Na-Al layers.<sup>7,8</sup> Scanning tunneling microscopy (STM) also revealed that surface alloys are formed on Au(111) by Na adsorption for  $c(4 \times 2)$  and  $(13 \times 13)$  structures.<sup>9</sup>

On fcc(001),  $(2 \times 1)$  and  $(3 \times 1)$  structures were found for K/Ag(001) and they are interpreted to consist of missing rows.<sup>10</sup> Other examples were found for K on Au(001) (Ref. 11) and Li on Cu(001).<sup>12</sup> We have determined by LEED analysis that the Cu(001)- $(2 \times 1)$ -Li structure also consists of a missing-row-type reconstruction of the top Cu layer, Li atoms being located in the missing-row sites.<sup>13</sup> In addition to such missing-row formation, it was found that anomalous  $(3 \times 3)$  and  $(4 \times 4)$  LEED patterns occur with increasing coverage, and these were proposed to be surface alloys.<sup>12</sup> For K/Au(001),  $c(8 \times 2)$  and  $(6 \times 2)$  structures were formed with further K deposition on the  $(2 \times 1)$  structure.<sup>11</sup> A  $c(2 \times 2)$  structure is formed for Na adsorption on Al(001) and its

structural model has been proposed to be a double layer consisting of an Al layer on a Na layer on Al(001), on the basis of a SEXAFS analysis.<sup>14</sup>

As summarized above, it is common for some fcc-metal-AM adsorption systems to have simple structures of missing rows or substitutional adsorption at low coverages, followed by complex structures with rather large unit cells at higher coverages. The simple structures are formed by substitution and ordering: Each adatom removes one or more substrate atoms and occupies the vacant site, forming a compositional unit that can order with increasing coverage. This growth mode has been confirmed by using STM for K on Cu(110).<sup>15</sup> It is important to analyze the complex structures seen at higher coverages, as their large unit cells could possibly indicate that a different type of structure is forming. Thus, for Li on Cu(001), the  $(2 \times 1)$  structure changes into  $(3 \times 3)$  and  $(4 \times 4)$ .<sup>12</sup> These have been proposed to be new types of surface alloys.<sup>8,12</sup> The recent development of the automated tensor LEED scheme makes it possible now to analyze such complex structures. We have chosen to study the Cu(001)- $(3 \times 3)$ -Li structure, the result of which, as we shall see, is very different from both the known simple structures and the proposed models for complex structures.

The experiments were carried out in a three-level UHV chamber equipped with standard facilities for surface science.<sup>16</sup> Li atoms were deposited onto Cu(001) from a SAES dispenser at 300 K. The Li coverage, the ratio of the number density of Li adatoms to that of Cu atoms in the ideal top layer of Cu(001), was determined by comparing LEED patterns at low and at room temperatures, and from Li  $KVV$  Auger intensities.<sup>12</sup> The pressures were  $\sim 1 \times 10^{-10}$  and  $\sim 5 \times 10^{-11}$  Torr during Li deposition and measurement, respectively. Water in the chamber is the most active species for the Li-covered Cu surface<sup>16</sup> and its partial pressure was reduced to less than  $1 \times 10^{-12}$  Torr. After measurement of intensity-energy ( $I-V$ ) curves, no contamination was detected by Li  $KVV$  Auger electron spectroscopy, which is very sensitive to surface oxides and hydroxides, and the LEED  $I-V$  curves did not change. LEED spot intensities were measured with a computer-controlled auto-LEED system.<sup>17</sup>  $I-V$  curves

were taken at normal incidence with an energy range from 16 to 200 eV on a 1-eV grid. The cumulative energy range over the nine inequivalent beams is 813 eV. Normal incidence was achieved by using the horizontal-beam method,<sup>18</sup> in which two equivalent spots located in the horizontal direction are averaged. The sample temperature was 180 K during measurement.

Our automated tensor LEED program<sup>19</sup> was used to calculate  $I$ - $V$  curves for the  $(3 \times 3)$  structure models. Six phase shifts were used to calculate atomic scattering ( $l_{\max} = 5$ ). The real part of the inner potential was determined during the course of the theory-experiment fit. The damping was represented by an imaginary part of the potential of  $-5.0$  eV. We used 335 and 480 K for the Cu and Li Debye temperatures, respectively.<sup>20</sup>

A total of 23 structural models, shown in Fig. 1, were examined for Cu(001)- $(3 \times 3)$ -Li in the present study. These models are selected under the condition that the Li coverage is either  $\frac{4}{9}$  or  $\frac{5}{9}$  (Ref. 21) and the symmetry is  $p4mm$ . The possible range of Li coverage was obtained in a previous study.<sup>12</sup> Briefly, models 1–4 and model 16 correspond to Li overlayers, while the others involves reconstruction of the substrate. Model 21, a completely intermixed Cu-Li layer, was proposed as a possible structure in our previous study.<sup>12</sup> The automated search algorithm was directed by the Pendry  $R$  factor,  $R_p$ . At first, the dominant seven of the nine inequivalent beams

TABLE I. Optimized Pendry  $R$  factors,  $R_p$ , for the 23 models of Cu(001)- $(3 \times 3)$ -Li shown in Fig. 1.

Model	$R_p$	Number of structural parameters	Model	$R_p$	Number of structural parameters
1	0.52	7	13	0.20	10
2	0.50	7	14	0.28	11
3	0.47	8	15	0.48	12
4	0.49	8	16	0.64	8
5	0.37	8	17	0.47	10
6	0.45	8	18	0.55	10
7	0.29	9	19	0.35	10
8	0.35	10	20	0.44	11
9	0.45	9	21	0.43	9
10	0.41	10	22	0.44	10
11	0.40	10	23	0.29	11
12	0.42	10			

$[(1,0), (1,1), (\frac{1}{3}, 0), (\frac{2}{3}, 0), (\frac{1}{3}, \frac{1}{3}), (\frac{2}{3}, \frac{1}{3}), \text{ and } (\frac{2}{3}, \frac{2}{3})]$  were examined.  $R_p$  values corresponding to the different models for the  $(3 \times 3)$  structure are listed in Table I. In order to limit the number of structural parameters entering the theory-experiment fit, we only allowed for displacements of the Li and Cu atoms preserving the  $p4mm$  symmetry: these displacements can be parallel and/or perpendicular to the surface, depending on the atom location in the unit cell. The number of independent structural parameters

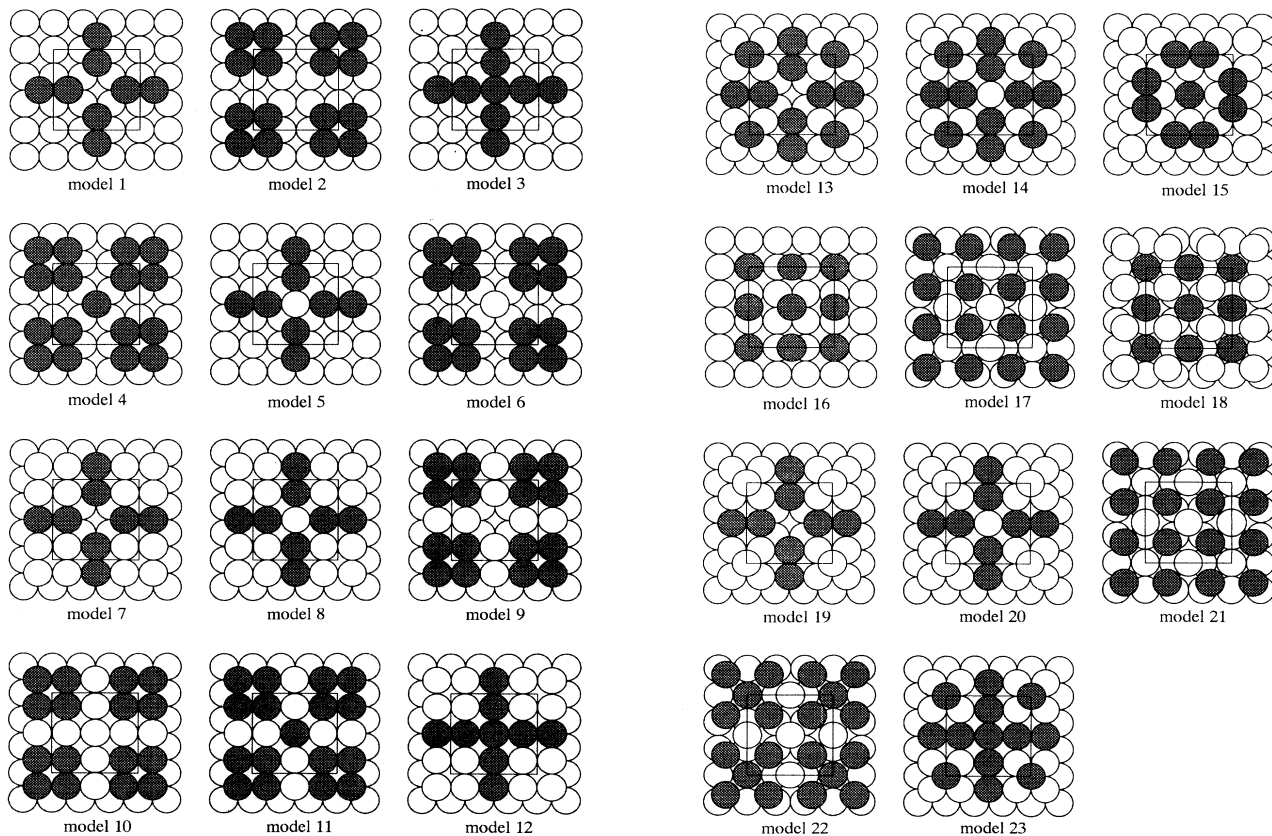


FIG. 1. Top views of the 23 examined models for the Cu(001)- $(3 \times 3)$ -Li structure. Dark-gray spheres are Li atoms, light-gray spheres represent Cu atoms in the first complete Cu layer, while blank spheres are Cu atoms above that layer. Squares indicate a  $(3 \times 3)$  unit cell.

used in the fit is also listed in Table I. The best fit occurs for model 13 and its  $R_p$  value is 0.20. Overlayer models and completely intermixed models can be ruled out because they have  $R_p$  values larger than 0.43.

Models 7, 14, and 23 have low  $R_p$  values of 0.29, 0.28, and 0.29, respectively. This is due to the fact that these structures are very similar to model 13 as seen in Fig. 1. The common features of these models are quartets of Cu atoms mutually joined by pairs of Li atoms. The differences concern the occupation of the remaining vacancies in the same layer, and the occupation of hollow sites above the quartets. Models 14 and 23 correspond to slightly different versions of model 13 and include Cu and Li atoms in the vacancy site, respectively. Their  $R_p$  values are worse than that of model 13, although the number of structural parameter is larger (in general, adding fit parameters improves the fit for the same model). Similarly, the  $R_p$  values of models 8 and 12 are higher than that of model 7. These results consistently suggest that the vacancy is indeed not filled.

Second, the large reduction of the  $R_p$  value from model 7 to model 13 leads to the conclusion that a Li atom site on the hollow site of the Cu quartet. This is further supported by the fact that the  $R_p$  values of models 14 and 23 are significantly lower than those of models 8 and 12, respectively. That model 13 is correct is also supported by the following check: when we use only fractional-order beams or only integer-order beams for optimization of model 13, the resulting  $I$ - $V$  curves of all beams are in good agreement with the experimental ones in either case. Further optimization has been carried out for model 13, including two additional beams  $[(1, \frac{1}{3})$  and  $(1, \frac{2}{3})]$ , and increasing  $l_{\max}$  to 6. The resulting  $R_p$  value is 0.19. In Fig. 2, the directions of lateral atomic displacements are indicated for best-fit model 13. The second complete Cu(001) plane was kept bulklike and its perpendicular position [shown as a line  $A-A'$  in the side view of Fig. 2(a)] is used as a reference plane for atomic heights (perpendicular positions) listed in Table II, together with the resulting interlayer spacings. The magnitudes of the lateral displacements are also given in Table II. The error bars were obtained from the variance of the  $R_p$  factor,  $\Delta R = R(8V_{0i}/\Delta E)^{1/2}$ , where  $R$  is the minimum  $R_p$  factor achieved,<sup>22</sup>  $V_{0i}$  is the imaginary part of the inner potential, and  $\Delta E$  is the total energy range. In Fig. 3, the calculated  $I$ - $V$  curves of the best-fit structure are compared with the experimental ones for the nine beams. Agreement between theory and experiment is rather good, and it should be emphasized that our best value  $R_p=0.19$  is excellent in comparison with those obtained for much less complicated yet related adsorption systems: the  $(2 \times 1)$  and  $c(2 \times 2)$  structures formed on Cu(001) upon Li adsorption at room and low temperatures, as recalculated by automated tensor LEED, give best-fit  $R_p$  values of 0.25 and 0.17, respectively.<sup>23</sup>

We emphasize some aspects of the best-fit structure (see Fig. 2 and Table II). First, the two Li atoms (numbered 2 in Fig. 2) in each pair joining adjacent Cu quartets (numbered 3) appear to move laterally in opposite directions away from the fourfold hollow sites in the un-

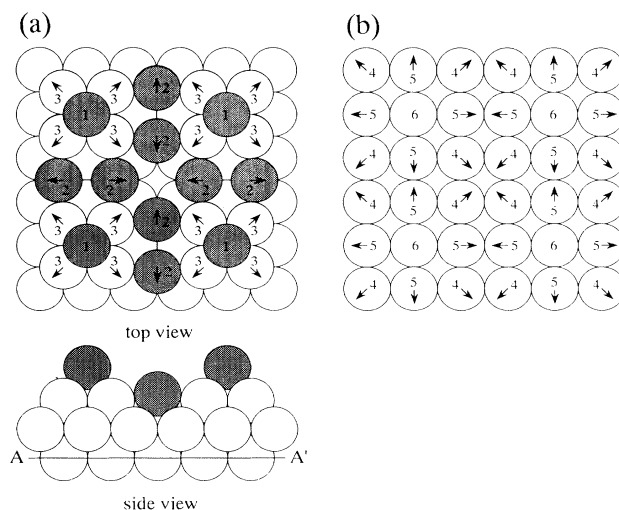


FIG. 2. (a) Top and side views of the best-fit Cu(001)-(3 $\times$ 3)-Li structure (model 13 in Fig. 1). Gray levels distinguish types of atoms as in Fig. 1. The numbers identify symmetrically equivalent atoms. Arrows indicate directions of displacements from ideal hollow sites. The line  $A-A'$  in the side view is the base line for heights shown in Table II. (b) Top view of the first complete Cu(001) layer (which lies just below the quartets), showing lateral relaxation directions.

derlying Cu(001) layer. The vacancies in the mixed layer accommodate these displacements. The distance between the two Li adatoms is  $3.15 \pm 0.52$  Å. The lateral positions are relatively uncertain, as usual in LEED near normal incidence. Nevertheless, this distance is in good agreement with the nearest-neighbor distance of Li adatoms in a saturated monolayer on Cu(001) at 180 K, namely, 3.07 Å. For comparison, the nearest-neighbor distance in bulk Li and the interatomic distance in the diatomic molecule  $\text{Li}_2$  are 3.02 and 2.67 Å, respectively.

Second, the height of the outermost Li atoms (numbered 1 in Fig. 2) above the Cu quartets is 1.91 Å, and this value is identical with the corresponding spacing between Li adatoms and the top Cu layer in Cu(001)-

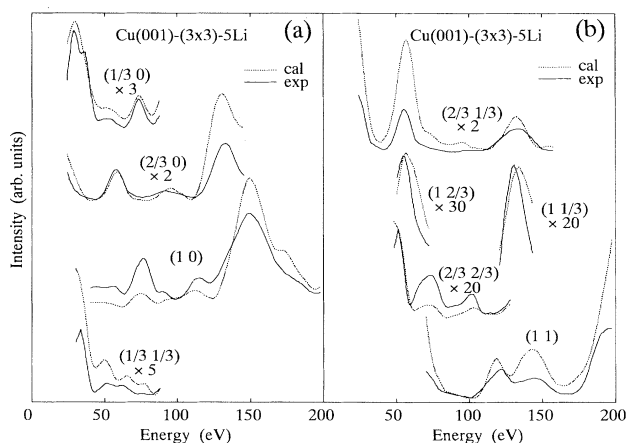


FIG. 3. Comparison between experimental (solid) and best-fit theoretical (dotted)  $I$ - $V$  curves for the Cu(001)-(3 $\times$ 3)-5 Li structure. Structural parameters for the best-fit structure shown in Fig. 2 are listed in Table II.

TABLE II. Optimum parameters of the best-fit structure for Cu(001)-(3×3)-Li illustrated in Fig. 2. Atomic numbers correspond to those in Fig. 2. Lateral displacements refer to displacements from hollow sites. Heights are measured from the plane A-A' in Fig. 2.

No.	Lateral displacement (Å)	Height (Å)	Interlayer spacing (Å)
1		5.38±0.07	
2	0.30±0.26	3.88±0.08	1.50
3	0.02±0.11	3.47±0.04	0.41
4	0.04±0.11	1.83±0.06	1.64
5	0.08±0.08	1.77±0.05	0.06
6	1.76±0.09		0.01

$c(2\times 2)$ -Li formed at 180 K, namely, 1.92 Å.<sup>23</sup> Third, the first complete Cu(001) layer is buckled and laterally relaxed. The Cu atoms numbered 5 and 6 are located at almost the same height, while the Cu atoms numbered 4 move outward significantly (0.06 Å). Fourth, the height of the Cu quartet above the average a plane of the first complete Cu layer is 1.67 Å. This is contracted by 7.5% from the bulk value (1.805 Å). It is interesting to note that this value is in good agreement with the interlayer spacing between the surface layer (containing the missing rows) and the first complete layer of Cu(001) in the Cu(001)-(2×1)-Li structure, 1.69 Å.

The best-fit Cu(001)-(3×3)-5 Li structure [with five Li atoms per (3×3) unit cell] is very different from other proposed, but as yet unsolved, surface AM alloys. It has been suggested that the Al(001)- $c(2\times 2)$ -Na structure consists of a  $c(2\times 2)$  Al layer on a  $c(2\times 2)$  Na layer on Al(001).<sup>14</sup> It has been proposed that the Al(111)-(2×2)-Na structure consists of intermixed double Na-Al layers<sup>8</sup> and that the Au(111)-(13×13)-Na structure has an intermixed incommensurate layer.<sup>9</sup> It should be emphasized again, however, that these models are not definitely determined yet. The Cu(001)-(3×3)-5 Li structure is the first to be determined among complicated surface alloys formed on metals by AM adsorption. In conclusion, the detailed complex surface structure of Cu(001)-(3×3)-5 Li has been shown to be strongly reconstructed, with partly Li-filled missing rows in the substrate and additional Li atoms above remaining Cu islands.

We thank Professor S. Nakanishi for informing us of his results on ion scattering experiments for the Cu(001)-Li(5×1) system before publication. This work was partially supported by a Grant-in-Aid (Grant No. 06452038) for Scientific Research from the Ministry of Education, Science and Culture of Japan and also by the Iketani Science and Technology Foundation. This work was also supported in part by the Director, Office of Energy Research, Office of Basic Energy Sciences, Materials Sciences Division, of the U.S. Department of Energy under Contract No. DE-AC03-76SF00098.

\*Author to whom all correspondence should be addressed.

FAX: +81-11-706-2916.

Electronic address: G13787%SIMAIL@JPNAC.BITNET or G13787@SINET.AD.JP

<sup>1</sup>B. E. Hayden, K. C. Prince, P. J. Davie, G. Paolucci, and A. M. Bradshaw, *Solid State Commun.* **48**, 325 (1983).

<sup>2</sup>R. J. Behm, in *Physics and Chemistry of Alkali Metal Adsorption*, edited by H. P. Bonzel, A. M. Bradshaw, and G. Ertl (Elsevier, Amsterdam, 1989), p. 111; C. J. Barnes, M. Lindroos, D. J. Holmes, and D. A. King, *ibid.*, p. 129.

<sup>3</sup>P. Häberle and T. Gustafsson, *Phys. Rev. B* **40**, 8218 (1989).

<sup>4</sup>S. Nakanishi, T. Yumura, K. Umezawa, H. Tochiwara, and S. Mizuno, *Phys. Rev. B* **49**, 4850 (1994).

<sup>5</sup>A. Schmalz, S. Sminpirooz, L. Becker, J. Haase, J. Neugebauer, M. Scheffler, D. R. Batchelor, D. L. Adams, and E. Bøgh, *Phys. Rev. Lett.* **67**, 2163 (1991).

<sup>6</sup>C. Stampfl, M. Scheffler, H. Over, J. Burchhardt, M. Nielsen, D. L. Adams, and W. Moritz, *Phys. Rev. Lett.* **69**, 1532 (1992).

<sup>7</sup>J. N. Andersen, M. Qvarford, R. Nyholm, J. F. van Acker, and E. Lundgren, *Phys. Rev. Lett.* **68**, 94 (1992).

<sup>8</sup>M. Kerkar, D. Fischer, D. P. Woodruff, R. G. Jones, R. D. Diehl, and B. Cowie, *Surf. Sci.* **278**, 246 (1992).

<sup>9</sup>J. V. Barth, H. Brune, R. Schuster, G. Ertl, and R. J. Behm, *Surf. Sci.* **292**, L769 (1993).

<sup>10</sup>M. Okada, H. Tochiwara, and Y. Murata, *Phys. Rev. B* **43**, 1411 (1991); *Surf. Sci.* **245**, 380 (1991).

<sup>11</sup>M. Okada, H. Iwai, R. Klauser, and Y. Murata, *J. Phys. Condens. Matter* **4**, L593 (1992).

<sup>12</sup>H. Tochiwara and S. Mizuno, *Surf. Sci.* **279**, 89 (1992).

<sup>13</sup>S. Mizuno, H. Tochiwara, and T. Kawamura, *Surf. Sci.* **292**, L811 (1993).

<sup>14</sup>S. Aminpirooz, A. Schmalz, L. Becker, N. Pangher, J. Haase, M. M. Nielsen, D. R. Batchelor, E. Bøgh, and D. L. Adams, *Phys. Rev. B* **46**, 15 594 (1992).

<sup>15</sup>R. Schuster, J. V. Barth, G. Ertl, and R. J. Behm, *Surf. Sci.* **247**, L229 (1991); *Phys. Rev. B* **44**, 13 689 (1991).

<sup>16</sup>S. Mizuno, H. Tochiwara, T. Kadowaki, H. Minagawa, K. Hayakawa, I. Toyoshima, and C. Oshima, *Surf. Sci.* **264**, 103 (1992); H. Tochiwara and S. Mizuno, *Chem. Phys. Lett.* **194**, 51 (1992).

<sup>17</sup>K. Müller and K. Heinz, in *Structural Studies of Surfaces*, edited by G. Höhler, Springer Series in Surface Sciences Vol. 2 (Springer, Berlin, 1985), p. 105.

<sup>18</sup>S. Mizuno, H. Tochiwara, and T. Kawamura, *J. Vac. Sci. Technol. A* **12**, 471 (1994).

<sup>19</sup>M. A. Van Hove, W. Mortiz, H. Over, P. J. Rous, A. Wander, A. Barbieri, N. Materer, U. Starke, and G. A. Somorjai, *Surf. Sci. Rep.* **19**, 191 (1993).

<sup>20</sup>S. Mizuno, H. Tochiwara, and T. Kawamura, *Surf. Sci.* **293**, 239 (1993).

<sup>21</sup>Exceptionally, the coverage of model 23 is  $\frac{6}{9}$ . This model, however, was examined tentatively to check serial structures, as discussed later.

<sup>22</sup>J. B. Pendry, *J. Phys. C* **13**, 937 (1980).

<sup>23</sup>S. Mizuno, H. Tochiwara, A. Barbieri, and M. A. Van Hove (unpublished).